Strong antiferromagnetic proximity coupling in the heterostructure superconductor $Sr_2VO_{3-\delta}FeAs$

Jong Mok Ok,[1,2,3,*] Chang Il Kwon,[1,2,*] O. E. Ayala Valenzuela,[1,4] Sunghun Kim,[5] Ross D. McDonald,[4] Jeehoon Kim,[1,2] E. S. Choi,[6] Woun Kang,[7] Y. J. Jo,[8] C. Kim,[9,10] E. G. Moon,[5] Y. K. Kim,[5] and Jun Sung Kim[1,2,†]

[1]*Center for Artificial Low Dimensional Electronic Systems, Institute for Basic Science, Pohang 37673, Korea*
[2]*Department of Physics, Pohang University of Science and Technology, Pohang 37673, Korea*
[3]*Department of Physics, Pusan National University, Busan 46241, Korea*
[4]*National High Magnetic Field Laboratory, Los Alamos National Laboratory, Los Alamos, New Mexico 87545, USA*
[5]*Department of Physics, Korea Advanced Institute of Science and Technology, Daejeon 34141, Korea*
[6]*National High Magnetic Field Laboratory, Florida State University, Tallahassee, Florida 32310, USA*
[7]*Department of Physics, Ewha Womans University, Seoul 120-750, Korea*
[8]*Department of Physics, Kyungpook National University, Daegu 41566, Korea*
[9]*Department of Physics and Astronomy, Seoul National University, Seoul 08826, Korea*
[10]*Center for Correlated Electron Systems, Institute for Basic Science, Seoul 08826, Korea*

(Received 3 October 2020; revised 26 February 2022; accepted 20 April 2022; published 6 June 2022)

We report the observation of strong magnetic proximity coupling in the heterostructure superconductor $Sr_2VO_{3-\delta}FeAs$, determined by upper critical field $H_{c2}(T)$ measurements up to 65 T. Using the resistivity and the radio-frequency measurements for both $H \parallel ab$ and $H \parallel c$, we found a strong upward curvature of $H_{c2}^{c}(T)$, together with a steep increase in $H_{c2}^{ab}(T)$ near T_c, yielding an anisotropic factor $\gamma_H = H_{c2}^{ab}/H_{c2}^{c}$ up to ~20, much higher than those of other iron-based superconductors. These are attributed to the Jaccarino-Peter effect, rather than to the multiband effect, due to strong exchange interaction between itinerant Fe spins of the FeAs layers and localized V spins of Mott-insulating $SrVO_{3-\delta}$ layers. These findings provide evidence for strong antiferromagnetic proximity coupling that is comparable to the intralayer superexchange interaction of the $SrVO_{3-\delta}$ layer and sufficient to induce magnetic frustration in $Sr_2VO_{3-\delta}FeAs$.

DOI: 10.1103/PhysRevB.105.214505

I. INTRODUCTION

Heterostructures of strongly correlated electronic systems offer novel and versatile platforms for triggering various types of exotic electronic orders [1–13]. When one of the constituent layers hosts an itinerant electron system, the other layer serves as an active spacer, introducing additional proximity coupling, and determines the ground state and the dimensionality of correlated heterostructures. For example, in high-T_c cuprates and iron-based superconductors (FeSCs), the proximity-coupled layers are found to be effective in changing the doping level, modifying the interlayer hopping strength, introducing lattice strain [1–5], and inducing an additional pairing interaction through interfacial phonons [6,7] or charge transfer [8,9]. Unlike the effects of charge or lattice degrees of freedom, magnetic proximity coupling has often been considered weak and thus to play a secondary role [10–13]. Possible strong magnetic proximity coupling, comparable to the intralayer magnetic interaction, may lead to unprecedented electronic phases, which have not been explored much experimentally.

$Sr_2VO_{3-\delta}FeAs$ is a naturally assembled heterostructure and has a unique position among FeSCs because of the possible strong magnetic proximity coupling [14]. In this compound, superconducting FeAs layers and insulating $SrVO_{3-\delta}$ layers are alternately stacked [15,16] [Fig. 1(a)], analogous to the superlattice of $FeSe/SrTiO_3$ [17,18], but with additional magnetic proximity coupling between Fe and V spins. The $SrVO_{3-\delta}$ layers have been identified to be in the Mott-insulating state [16,19–22] but do not trigger a long-range magnetic transition [16]. Instead, in the FeAs layers, various electronic phase transitions occur above the superconducting transition at $T_c \sim 30$ K [15,16,23], including a mysterious C_4-symmetric transition at $T_0 \sim 150$ K [16,24–26] without a signature of breaking underlying symmetries [27]. Such a transition has not been observed in other correlated heterostructures, and magnetic proximity coupling that induces frustration between stripe-type Fe antiferromagnetism and Neel-type V antiferromagnetism has been suggested as the possible reason [16]. However, whether the magnetic proximity coupling is strong enough and, if so, what type it is, ferromagnetic (FM) or antiferromagnetic (AFM), have remained elusive.

In this work, we present experimental evidence of strong AFM exchange coupling of itinerant Fe spins coupled to localized V spins using the upper critical field H_{c2} of the $Sr_2VO_{3-\delta}FeAs$ single crystal for both $H \parallel ab$ and $H \parallel c$, determined by magnetoresistance measurements up to 30 T and radio-frequency (rf) contactless measurements up to 65 T. A strongly convex $H_{c2}^{c}(T)$ for $H \parallel c$ is observed, in contrast to

*These authors contributed equally to this work.
†js.kim@postech.ac.kr

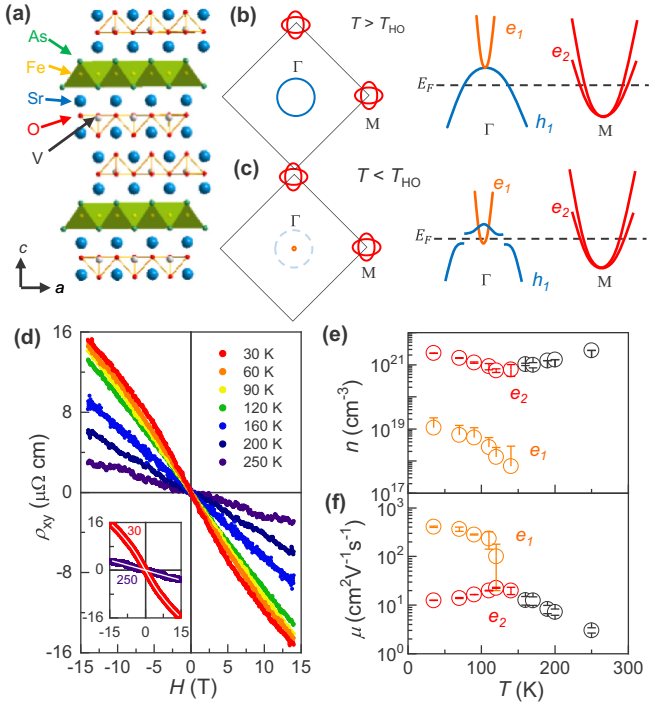

FIG. 1. (a) Crystal structure of $Sr_2VO_{3-\delta}FeAs$ consisting of FeAs layers and $SrVO_{3-\delta}$ layers. Schematic illustrations of the Fermi surface and band structures (b) above and (c) below $T_0 = 150$ K. (d) Magnetic field dependence of the Hall resistivity $\rho_{xy}(H)$ measured at different temperatures. The white solid lines in the inset represent best fits for Hall data. Temperature dependence of (e) the carrier density and (f) the mobility, extracted from the fits using the one-band model (black) for $T > T_0$ and the two-band model (red and orange) for $T < T_0$.

the steep linear increase of $H_{c2}^{ab}(T)$ near T_c for $H \parallel ab$. In comparison with other FeSCs, we found that the Jaccarino-Peter (JP) effect with an exchange field up to ~20 T is responsible for this unusual behavior. Our observations confirm that magnetic proximity coupling can play a critical role in inducing the unusual magnetic and superconducting properties of $Sr_2VO_{3-\delta}FeAs$.

II. EXPERIMENTS

Single crystals of $Sr_2VO_{3-\delta}FeAs$ were grown using self-flux techniques [16]. The typical size of each single crystal was $200 \times 200 \times 10\ \mu m^3$. High crystallinity and stoichiometry were confirmed by x-ray diffraction and energy-dispersive spectroscopy. The single crystals show a clear superconducting transition at $T_c^{onset} \sim 27$ K, which is somewhat lower than the maximum $T_c^{onset} \sim 35$ K in a polycrystalline sample [15]. This difference may be attributed to the partial deficiency of oxygen [28]. Magnetotransport measurements were carried out using the conventional six-probe method in a 14 T physical property measurement system and a 33 T Bitter magnet at the National High Magnetic Field Laboratory, Tallahassee. rf contactless measurements up to 65 T were performed at the National High Magnetic Field Laboratory, Los Alamos.

III. RESULTS

A. Fermi surface reconstruction

Before discussing the upper critical field H_{c2} of $Sr_2VO_{3-\delta}FeAs$, we first consider the Fermi surface (FS) reconstruction across the C_4-symmetric transition $T_0 \approx 150$ K. According to recent angle-resolved photoemission spectroscopy (ARPES) results for $Sr_2VO_{3-\delta}FeAs$ in a wide range of temperatures, the heavy-hole FS centered at the Γ point of Brillouin zone (BZ), denoted h_1 in Figs. 1(b) and 1(c), has a relatively strong k_z dispersion and becomes fully gapped below T_0 [27]. In contrast, the two-dimensional electron FS at the M point [e_2 in Figs. 1(b) and 1(c)] remains gapless [27]. Concomitantly, the additional small electron FS [e_1 in Figs. 1(b) and 1(c)], which is absent in the calculated band structures of $Sr_2VO_{3-\delta}FeAs$, is introduced at the Γ point, as illustrated in Figs. 1(b) and 1(c). Because of this unusual band-selective gap opening at T_0, low-energy electronic structures of $Sr_2VO_{3-\delta}FeAs$ are significantly reconstructed, yielding two separate electron FSs (e_1 and e_2) with a strong mismatch in size, as shown in Fig. S1 in the Supplemental Material [29] (see also Refs. [30–45] therein). These features are highly distinct from those of other FeSCs. The FS reconstruction of $Sr_2VO_{3-\delta}FeAs$ is also probed by the field-dependent Hall resistivity $\rho_{xy}(H)$ of $Sr_2VO_{3-\delta}FeAs$ at different temperatures under magnetic field up to 14 T [Fig. 1(d)]. Above $T_0 \sim 150$ K, a linear field dependence of $\rho_{xy}(H)$ with a negative slope is observed up to $H = 14$ T, similar to the cases of other FeSCs, in which charge conduction is dominated by electron FSs with high mobility [46]. The contribution of the hole FSs usually appears in $\rho_{xy}(H)$ at low temperatures with a positive slope [29,47–52] but is completely absent in $Sr_2VO_{3-\delta}FeAs$.

Instead, we found that a nonlinear field dependence in $\rho_{xy}(H)$ suddenly appears below T_0, which is well reproduced by the two-band model with two distinct electron carriers. Using the constraint $1/\rho_{xx}(T) = \sum n_i e \mu_i$, the fit to the two-band model gives us the temperature-dependent carrier density n_i and carrier mobility μ_i, as shown in Figs. 1(e) and 1(f). Clearly, additional electron carriers e_1 with lower density but higher mobility are induced on top of the high-density electron carriers (e_2). The densities of the two electron carriers are estimated to be $\approx 1.1 \times 10^{19}$ and $\approx 2.3 \times 10^{21}$ cm^{-3}, which are in good agreement with the values for the e_1 FS at Γ ($\approx 2.0 \times 10^{19}$ cm^{-3}) and the e_2 FS at the X point ($\approx 1.1 \times 10^{21}$), obtained in recent ARPES studies [22]. This additional conduction channel of the small FS (e_1) with high mobility compensates for the loss of conduction from the gapped hole FS below T_0, which may explain the weak resistivity anomaly across T_0.

B. Upper critical fields

Now we focus on the upper critical field H_{c2} of $Sr_2VO_{3-\delta}FeAs$ single crystals, obtained from the rf measurements and the resistivity (Fig. 2). The radio-frequency curves as a function of magnetic fields along $H \parallel ab$ and $H \parallel c$ yield $H_{c2}(T)$ at various temperatures [Figs. 2(a) and 2(b)]. Here we determined H_{c2} by taking the magnetic field at which the steepest slope of the radio-frequency intercepts the

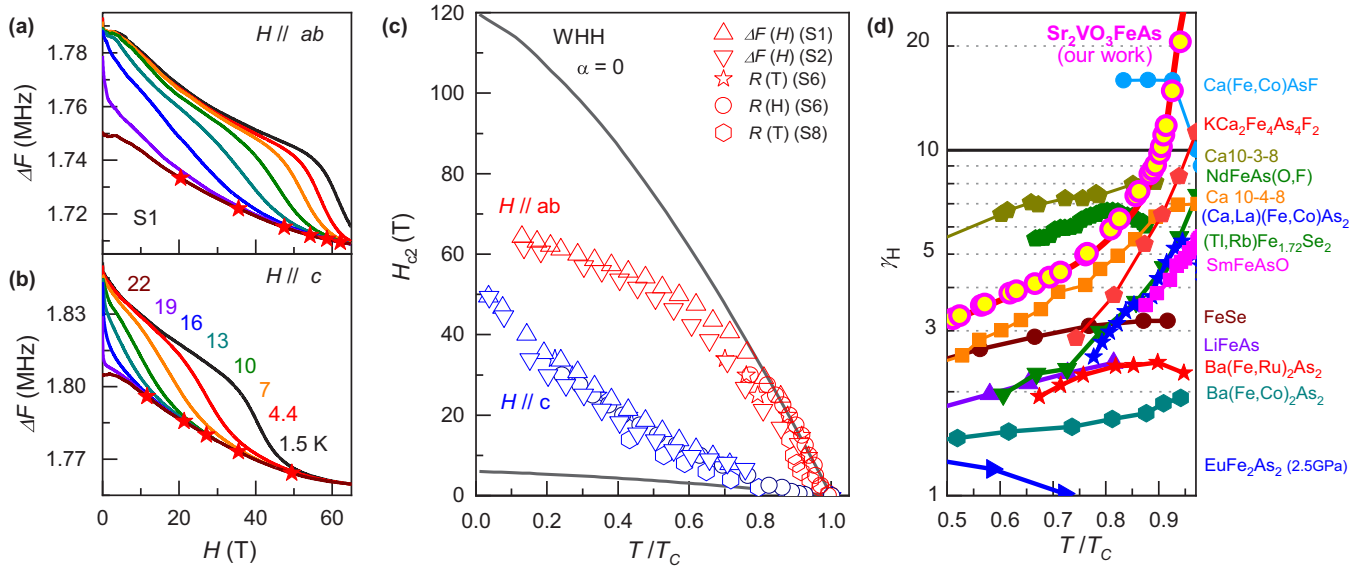

FIG. 2. Magnetic field dependence of the radio-frequency for (a) $H \parallel ab$ and (b) $H \parallel c$. Red stars show the estimated H_{c2}. (c) Upper critical field $H_{c2}(T)$ for $H \parallel ab$ (red symbols) and $H \parallel c$ (blue symbols) as a function of the normalized temperature T/T_c for the four crystals (S1, S2, S6, S8) estimated from the tunnel diode oscillator and resistivity measurements. Black solid lines are Werthamer-Helfand-Hohenberg curves with $\alpha = 0$. (d) Temperature-dependent anisotropic factor γ_H of $Sr_2VO_{3-\delta}FeAs$ and other FeSCs [53–64]. The red solid line shows γ_H of $Sr_2VO_{3-\delta}FeAs$ calculated from the $H_{c2}(T)$ fits for comparison.

normal-state background. The temperature and magnetic field dependences of the resistivity ρ_{xx} were also used to determine $H_{c2}(T)$ under magnetic field up to 33 T (Supplemental Material, Fig. S2) [29]. Using the criterion of 50% resistive transition, we obtained $H_{c2}(T)$ consistent with that from the rf contactless measurements. We note that using different criteria for H_{c2} in the rf and the resistivity measurements led to qualitatively the same $H_{c2}(T)$ behavior (Supplemental Material, Fig. S3) [29].

Figure 2(c) shows $H_{c2}(T)$ curves as a function of the normalized temperature ($t = T/T_c$) for $H \parallel ab$ and $H \parallel c$. We found that $H_{c2}(T)$ curves taken from different samples and different measurements are consistent with each other. Depending on the magnetic field orientations, $H_{c2}(T)$ exhibits different behaviors. For $H \parallel ab$, $H^{ab}_{c2}(T)$ shows a concave temperature dependence with saturation at low temperatures. This shape is typically observed in many FeSCs [65,66], in which the Pauli limiting effect dominates over other pair-breaking mechanisms. In contrast, $H^{c}_{c2}(T)$ for $H \parallel c$ shows a strongly convex behavior with a strong upward curvature. Similar convex behaviors of $H_{c2}(T)$ have been rarely observed, except in some FeSCs, including $Ba(Fe,Co)_2As_2$ [53], $(Sr,Eu)(Fe,Co)_2As_2$ [67], LaFeAs(O,F) [68], and NdFeAs(O,F) [54]. However, their upward curvature of $H_{c2}(T)$ is far less significant than that found in $Sr_2VO_{3-\delta}FeAs$.

This strong anisotropic behavior of H_{c2} in $Sr_2VO_{3-\delta}FeAs$ can be quantified by the anisotropy factor $\gamma_H = H^{ab}_{c2}/H^{c}_{c2}$. We plot the temperature-dependent γ_H for $Sr_2VO_{3-\delta}FeAs$ together with other FeSCs in Fig. 2(d). Near T_c, the slope of $H_{c2}(T)$ is estimated to be $dH_{c2}/dT|_{T_c} \simeq -7.4$ T/K for $H \parallel ab$ and $\simeq -0.2$ T/K for $H \parallel c$ in $Sr_2VO_{3-\delta}FeAs$. These values lead to $\gamma_H \sim 20$ at $T \approx T_c$, much higher than those found in FeSCs. As shown in Fig. 2(d), the typical values of γ_H are $\simeq$ 2–3 in the so-called 122 compounds, and $\gamma_H \simeq$ 5–6 in the 1111 compounds. Usually, a thicker blocking layer between the superconducting layers induces the stronger anisotropy of H_{c2} with a larger γ_H. The γ_H values of various FeSCs with different thicknesses d of the blocking layer follow the empirical relation $\gamma_H/d \sim 0.65$ Å^{-1} (Supplemental Material, Fig. S4) [29]. However, $Sr_2VO_{3-\delta}FeAs$ has $\gamma_H \approx 20$, far larger than what is expected, which suggests that the relatively thick blocking layer in $Sr_2VO_{3-\delta}FeAs$ alone cannot explain the observed γ_H and its strong temperature dependence. Recently, new members of the FeCS family, Ca(Fe,Co)AsF [69] and $KCa_2Fe_4As_4F_2$ [70], were found to show a large γ_H near T_c, comparable to that of $Sr_2VO_{3-\delta}FeAs$ near T_c. In these FeSCs, the steep slope of the upper critical field $H^{ab}_{c2}(T)$ for $H \parallel ab$, as compared to the moderate one of $H^{c}_{c2}(T)$ for $H \parallel c$, is responsible for the large γ_H. When the superconductivity approaches the two-dimensional limit, $H^{ab}_{c2}(T) \sim (1 - T/T_c)^{1/2}$, and $H^{c}_{c2}(T) \sim (1 - T/T_c)$ near T_c, leading to the diverging behavior of γ_H near T_c, which is nicely demonstrated by $KCa_2Fe_4As_4F_2$ [70]. However, in $Sr_2VO_{3-\delta}FeAs$, the large γ_H and its strong temperature dependence are due to the strong upward curvature of $H^{c}_{c2}(T)$ and its low slope near T_c for $H \parallel c$. Thus, the temperature dependences of $H_{c2}(T)$ for $H \parallel ab$ and $H \parallel c$ are highly distinct from those of other FeSCs, indicating that the superconducting properties of $Sr_2VO_{3-\delta}FeAs$ are exceptional among FeSCs.

For a detailed comparison with other FeSCs, we plot the slopes of the upper critical fields dH_{c2}/dT near T_c for both $H \parallel ab$ and $H \parallel c$ in Fig. 3. In the case of $H \parallel ab$, the normalized slope of the upper critical field at T_c, $-(dH^{ab}_{c2}/dT)/T_c$ is closely related to the diffusivity along the c axis and thus is sensitive to the interlayer distance. $Sr_2VO_{3-\delta}FeAs$ nicely follows the linear trend of $-(dH^{ab}_{c2}/dT)/T_c$ as a function of the thickness of the blocking layer d [Fig. 3(a)]. The distinct

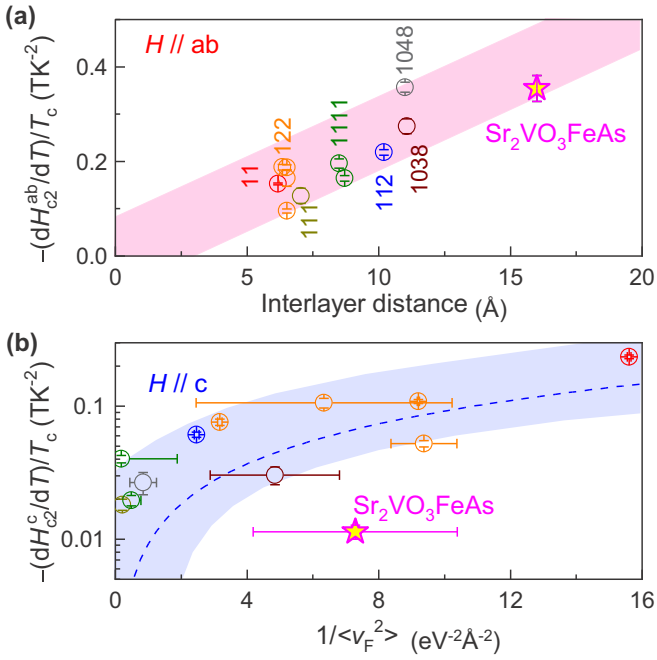

FIG. 3. (a) Interlayer distance dependence of the normalized slope of $H_{c2}(T)$ near T_c for $H \parallel ab$. The normalized slope of $H_{c2}(T)$ increases in proportion to the interlayer distance. (b) Normalized slope of $H_{c2}(T)$ near T_c for $H \parallel c$ as a function of $\langle v_F^2 \rangle$, which is estimated from ARPES results [22,71–79].

behavior of $Sr_2VO_{3-\delta}FeAs$ is observed for $H \parallel c$. In the case of $H \parallel c$, $-(dH_{c2}^c/dT)/T_c$ is more sensitive to the electronic structure of the FeAs layer than to the interlayer distance. In conventional superconductors, $-(dH_{c2}^c/dT)/T_c$ is known to be proportional to $1/\langle v_F^2 \rangle$ [Fig. 3(b), blue dashed line]. The normalized slope $-(dH_{c2}^c/dT)/T_c$ obtained for various FeSCs shows a strong correlation with $1/\langle v_F^2 \rangle$, estimated from the ARPES results [22,71–79] [Fig. 3(b)]. The data for $Sr_2VO_{3-\delta}FeAs$, however, clearly deviate from this trend and show the lowest $-(dH_{c2}^c/dT)/T_c$ value, leading to the largest γ_H among the FeSCs.

C. Strong proximity coupling

For many FeSCs, temperature-dependent $H_{c2}^c(T)$ has been understood using the two-band dirty-limit model [80]. In this model, the intra- and interband couplings ($\lambda_{11,22}$ and $\lambda_{12,21}$) and the diffusivity of each band (D_1, D_2) determine $H_{c2}^c(T)$ (see the Supplemental Material, Fig. S5) [29]. The two-band model can also reproduce the strongly convex behavior of $H_{c2}^c(T)$ of $Sr_2VO_{3-\delta}FeAs$ if we assume dominant interband coupling ($\lambda_{11}\lambda_{22} < \lambda_{12}\lambda_{21}$) and an unusually large $\eta = D_1^{ab}/D_2^{ab} \sim 30$ (Supplemental Material, Figs. S5 and S6) [29]. We note, however, that most of the FeSCs show a concave $H_{c2}^c(T)$, and even in a few cases, like $Ba(Fe, Co)_2As_2$ [53], LaFeAs(O,F) [68], and NdFeAs(O,F) [54], that show a convex $H_{c2}^c(T)$, the highest estimated η is ~10 [66], which is far less than the estimated $\eta \sim 30$ for $Sr_2VO_{3-\delta}FeAs$. Furthermore, the hole FS (h_1) centered at the Γ point of the BZ is gapped out below T_0 [Figs. 1(b) and 1(c)] and therefore cannot participate in the interband superconducting pairing. The remaining interband coupling channel is between electron FSs (e_1 and e_2) centered at the Γ and M points [Fig. 1(c)]. However, considering their drastic size difference of two orders of magnitude, confirmed by ARPES and Hall resistivity results, they are unlikely to produce strong interband coupling. These observations suggest that the conventional multiband effect cannot be the origin of the observed $H_{c2}^c(T)$ of $Sr_2VO_{3-\delta}FeAs$.

Instead, magnetic coupling between itinerant Fe and localized V spins can offer a natural explanation for the strongly convex behavior of $H_{c2}^c(T)$. Recent high-field magnetoresistance (MR) results revealed a strong negative MR with a clear kink at ~38 T for $H \parallel c$, in contrast to the monotonic positive MR for $H \parallel ab$ [27]. These results resemble the case of $EuFe_2As_2$ [81] and indicate a field-induced saturation of the magnetic V moment for $H \parallel c$ but not for $H \parallel ab$. Strong exchange coupling J of itinerant Fe electrons with localized V spins is then expected to introduce a net internal magnetic field $H_J = J\langle S \rangle / g_m \mu_B$, which is referred to as the JP effect [82]. With the AFM exchange interaction ($J < 0$), a negative H_J is produced by polarization of V spins along the external field, particularly for $H \parallel c$. For paramagnetic V spins, their susceptibility and thus H_J increase with decreasing temperature. Therefore, H_J compensates for the external field and enhances $H_{c2}(T)$ at low temperature in the presence of large external fields. This trend results in a convex $H_{c2}(T)$, as observed in Fig. 2(c).

In the JP model with multiple pair breakings, including the exchange field due to the localized moments [82], $H_{c2}(T)$ can be described as

$$\ln\frac{1}{t} = \left(\frac{1}{2} + \frac{i\lambda_{SO}}{4\gamma}\right) \times \Psi\left(\frac{1}{2} + \frac{h + i\lambda_{SO}/2 + i\gamma}{2t}\right) + \left(\frac{1}{2} - \frac{i\lambda_{SO}}{4\gamma}\right) \times \Psi\left(\frac{1}{2} + \frac{h + i\lambda_{SO}/2 - i\gamma}{2t}\right) - \Psi\left(\frac{1}{2}\right), \quad (1)$$

where $\gamma = [\alpha^2(h + h_J)^2 - \lambda_{SO}^2]^{\frac{1}{2}}$, $t = T/T_c$, $h = 0.281 H_{c2}/H_{c2}^*$, $h_J = 0.281 H_J/H_{c2}^*$, H_{c2}^* is the orbital critical field at $T = 0$ K, Ψ is the digamma function, λ_{SO} is the spin-orbit scattering parameter, and α is the Maki parameter [83]. The orbital critical field H_{c2}^* is estimated from the slope $(dH_{c2}/dT)|_{T_c}$ [Fig. 2(c)] as $H_{c2}^* = -0.69 T_c (dH_{c2}/dT)|_{T_c}$, and the typical values of $\alpha = 4$ and $\lambda_{SO} = 0$ are assumed, as widely done for other Fe-based superconductors [84,85]. Here the temperature and field dependence of the net internal magnetic field $H_J(H, T)$ should follow the susceptibility data for the V spins of $Sr_2VO_{3-\delta}FeAs$. As confirmed by a previous V NMR study [16], V local spins remain in the paramagnetic state at low temperatures with finite antiferromagnetic interaction, for which the strength is estimated by the Curie-Weiss temperature $\Theta_{CW} = -110$ K for $H \parallel c$ and $\Theta_{CW} = -119$ K for $H \parallel ab$ from the magnetic susceptibility [16]. Therefore, the temperature and field dependence of V magnetic moments M follows the Curie-Weiss law, $M(H, T) \propto H/(T - \Theta_{CW})$, and thus, $H_J(H, T)$ is described by $H_J(H, T) = \lambda_J M(H, T)$, where λ_J is a factor proportional to the exchange coupling J of itinerant Fe electrons and localized V spins. Using a

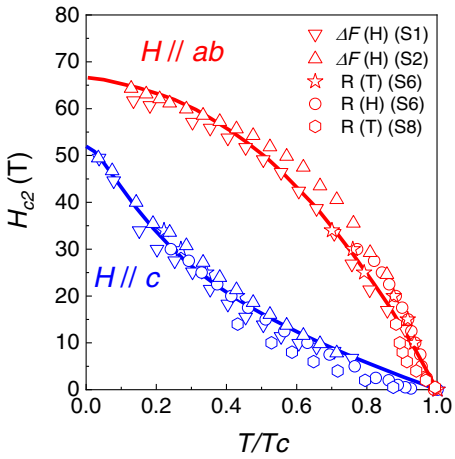

FIG. 4. Temperature-dependent upper critical field $H_{c2}(T)$ of $Sr_2VO_{3-\delta}FeAs$ for both $H \parallel ab$ and $H \parallel c$. Red and blue solid lines are Jaccarino-Peter fits for $H \parallel ab$ and $H \parallel c$, respectively.

temperature-independent λ_J as the only fitting parameter, we nicely reproduce the temperature-dependent $H_{c2}(T)$ of $Sr_2VO_{3-\delta}FeAs$ for $H \parallel c$ and $H \parallel ab$, as shown in Fig. 4. The coupling constant λ_J and H_J at H_{c2} and zero temperature are listed in Table I. The good agreement between experiments and calculations strongly suggests that the interlayer coupling between local V spins and itinerant Fe spins can explain the characteristic temperature-dependent $H_{c2}(T)$ of $Sr_2VO_{3-\delta}FeAs$ for $H \parallel c$ and $H \parallel ab$ (Supplemental Material, Fig. S7) [29].

IV. DISCUSSION

The maximum $H_J \approx -22$ T for $Sr_2VO_{3-\delta}FeAs$, obtained for $H \parallel c$, is comparable to those of other superconductors, including $EuMo_6S_8$ [86,87] and λ-(BETS)$FeCl_4$ (BETS = bis(ethylenedithio)tetraselenafulvalene) [88,89], and far lower than $H_J \sim -70$ T for $EuFe_2As_2$ [81]. Sizable anisotropies in H_J and λ_J are observed between the cases of $H \parallel c$ and $H \parallel ab$ (Table I). The origin of such anisotropy remains unclear, but similar behavior has been observed in the case of $EuFe_2As_2$ [81]. For $H \parallel c$, we found that the magnetic interlayer coupling constant $J \sim 2.3$ meV, estimated from H_J, is similar in $EuFe_2As_2$ and $Sr_2VO_{3-\delta}FeAs$, considering the smaller $\langle S \rangle = 1$ of V spins with $3d^2$ configurations compared with $\langle S \rangle = 7/2$ for Eu spins. This observation suggests that they gave similar interlayer couplings between itinerant electrons in the FeAs layers and localized spins in the adjacent layers. Despite the similarity, the magnetism of $Sr_2VO_{3-\delta}FeAs$ is highly distinct from that of $EuFe_2As_2$. In $EuFe_2As_2$, Eu magnetism is induced by the Ruderman-Kittel-Kasuya-Yosida (RKKY) interaction due to itinerant Fe electrons [90]. In contrast, the $SrVO_{3-\delta}$ layers in $Sr_2VO_{3-\delta}FeAs$ are in the Mott-insulating state, and the localized V spins are coupled through their intralayer superexchange interaction J_S, competing with the RKKY interaction through the FeAs layers. The interlayer magnetic coupling strength of $J \sim 2.3$ meV in $Sr_2VO_{3-\delta}FeAs$ is comparable to the superexchange interaction of V spins, $J_S \sim 1.6$ meV, estimated from the Curie-Weiss temperature $\Theta_{CW} = -110$ K [16].

The consequences of the strong AFM proximity coupling in $Sr_2VO_{3-\delta}FeAs$ are highly unusual. Without it, the $SrVO_{3-\delta}$ layer in the Mott-insulating state would likely host Neel-type AFM order, and the FeAs layer would have stripe-type AFM order [91]. However, due to the strong proximity coupling, two inherent magnetic instabilities in each layer are frustrated, which may destabilize these conventional AFM orders in subsystems. The unusual paramagnetism of the V spins, stabilizing far below $\Theta_{CW} \sim 100$ K, and the spin gap behavior of the Fe spins, developing near ~200 K [16], are signatures of this magnetic frustration. Furthermore, recent high-field transport experiments [27] revealed that the anisotropic magnetoresistance is developed below the mysterious C_4-symmetric transition at $T_0 \sim 150$ K. This indicates spin scattering between the itinerant Fe and localized V spins below T_0, consistent with the observed strong magnetic proximity coupling in this work. While the nature and origin of the C_4-symmetric transition at T_0 in $Sr_2VO_{3-\delta}FeAs$ remain to be clarified, these observations highlight the dominant role of magnetic proximity coupling in triggering an exotic electronic order, which is not present in each subsystem. A detailed microscopic understanding of proximity magnetic coupling, particularly its anisotropic nature, is highly desirable.

V. CONCLUSION

Our findings on strong magnetic proximity coupling have considerable relevance in the fields of strongly correlated heterostructures, beyond $Sr_2VO_{3-\delta}FeAs$. Common wisdom states that for the Mott-insulating system, additional magnetic coupling across the interface with an itinerant electron system is weak and usually leads to a small perturbation to its dominant intralayer magnetic interaction [10–13]. In contrast, $Sr_2VO_{3-\delta}FeAs$ establishes an example in which the magnetic proximity coupling competes on equal footing with the intralayer magnetic interactions in strongly correlated heterostructures. Our work thus demonstrates that proper design and synthesis of heterostructures of correlated itinerant and

TABLE I. Maximum H_J and λ_J of $Sr_2VO_{3-\delta}FeAs$ for both directions compared to other materials.

	T_c (K)	$\lvert H_J^{ab}\rvert$ (T)	$\lvert H_J^{c}\rvert$ (T)	$\lvert \lambda_J^{ab}\rvert$	$\lvert \lambda_J^{c}\rvert$
Sr_2VO_3FeAs	30	19.5	22.3	141	204
$EuFe_2As_2$ [81]	30	168	70	187	83
$EuMo_6S_6$ [86,87]	12		38		383
λ-(BETS)$FeCl_4$ [88,89]	4.2		32		813

Mott-insulating electron systems can offer a promising material platform to study exotic phases stabilized by frustration of the competing interactions of subsystems and can lead to rich physics triggered by dominant magnetic proximity coupling.

ACKNOWLEDGMENTS

The authors thank Y. K. Bang for fruitful discussions. We also thank H. G. Kim at Pohang Accelerator Laboratory (PAL) for the technical support. This work was supported by the Institute for Basic Science (IBS) through the Center for Artificial Low Dimensional Electronic Systems (Gran No. IBS-R014-D1) and by the National Research Foundation of Korea (NRF) through SRC (Grant No. 2018R1A5A6075964) and the Max Planck-POSTECH Center for Complex Phase Materials (Grant No. 2016K1A4A4A01922028). W.K. acknowledges the support from NRF (Grants No. 2018R1D1A1B07050087 and 2018R1A6A1A03025340), and Y.J.J. was supported by NRF (Grant No. NRF-2019R1A2C1089017). J.M.O. acknowledges support from the Korea Basic Science Institute (National research Facilities and Equipment Center) grant funded by the Ministry of Education (Grant No. 2021R1A6C101A429) and the National Research Foundation of Korea (NRF) (Grant No. 2021R1F1A1056934). C.K. acknowledges support from IBS-CCES (Grant No. IBS-R009-G2). E.G.M. acknowledges the support from NRF (Grants No. NRF-2019M3E4A1080411, No. NRF-2020R1A4A3079707, and No. NRF-2021R1A2C4001847). A portion of this work was performed at the National High Magnetic Field Laboratory, which is supported by National Science Foundation Cooperative Agreement No. DMR-1644779 and the state of Florida.

[1] A. Damascelli, Z. Hussain, and Z.-X. Shen, Rev. Mod. Phys. **75**, 473 (2003).

[2] J. Chakhalian, J. W. Freeland, G. Srajer, J. Strempfer, G. Khaliullin, J. C. Cezar, T. Charlton, R. Dalgliesh, C. Bernhard, G. Cristiani, H.-U. Habermeier, and B. Keimer, Nat. Phys. **2**, 244 (2006).

[3] A. Gozar, G. Logvenov, L. Fitting Kourkoutis, A. T. Bollinger, L. A. Giannuzzi, D. A. Muller, and I. Bozovic, Nature (London) **455**, 782 (2008).

[4] D. K. Satapathy *et al.*, Phys. Rev. Lett. **108**, 197201 (2012).

[5] N. Driza, S. Blanco-Canosa, M. Bakr, S. Soltan, M. Khalid, L. Mustafa, K. Kawashima, G. Christiani, H.-U. Habermeier, G. Khaliullin, C. Ulrich, M. Le Tacon, and B. Keimer, Nat. Mater. **11**, 675 (2012).

[6] J.-F. Ge, Z.-L. Liu, C. Liu, C.-L. Gao, D. Qian, Q.-K. Xue, Y. Liu, and J.-F. Jia, Nat. Mater. **14**, 285 (2015).

[7] J. J. Lee, F. T. Schmitt, R. G. Moore, S. Johnston, Y.-T. Cui, W. Li, M. Yi, Z. K. Liu, M. Hashimoto, Y. Zhang, D. H. Lu, T. P. Devereaux, D.-H. Lee, and Z.-X. Shen, Nature (London) **515**, 245 (2014).

[8] B. Lei, J. H. Cui, Z. J. Xiang, C. Shang, N. Z. Wang, G. J. Ye, X. G. Luo, T. Wu, Z. Sun, and X. H. Chen, Phys. Rev. Lett. **116**, 077002 (2016).

[9] W. S. Kyung, S. S. Huh, Y. Y. Koh, K.-Y. Choi, M. Nakajima, H. Eisaki, J. D. Denlinger, S.-K. Mo, C. Kim, and Y. K. Kim, Nat. Mater. **15**, 1233 (2016).

[10] V. Sunko, F. Mazzola, S. Kitamura, S. Khim, P. Kushwaha, O. J. Clark, M. D. Watson, I. Marković, D. Biswas, L. Pourovskii, T. K. Kim, T.-L. Lee, P. K. Thakur, H. Rosner, A. Georges, R. Moessner, T. Oka, A. P. Mackenzie, and P. D. C. King, Sci. Adv. **6**, 0611 (2020).

[11] J.-H. She, C. H. Kim, C. J. Fennie, M. J. Lawler, and E.-A. Kim, npj Quantum Mater. **2**, 64 (2017).

[12] N. Rohling, E. L. Fjaerbu, and A. Brataas, Phys. Rev. B **97**, 115401 (2018).

[13] E. L. Fjærbu, N. Rohling, and A. Brataas, Phys. Rev. B **100**, 125432 (2019).

[14] In order to emphasize the naturally assembled heterostructure, we used the term "$Sr_2VO_{3-\delta}FeAs$" rather than "$Sr_2VFeAsO_{3-\delta}$" following the international rule. See Z. Hiroi, arxiv:0805.4668.

[15] X. Zhu, F. Han, G. Mu, P. Cheng, B. Shen, B. Zeng, and H.-H. Wen, Phys. Rev. B **79**, 220512(R) (2009).

[16] J. M. Ok, S.-H. Baek, C. Hoch, R. K. Kremer, S. Y. Park, S. Ji, B. Büchner, J.-H. Park, S. I. Hyun, J. H. Shim, Y. Bang, E. G. Moon, I. I. Mazin, and J. S. Kim, Nat. Commun. **8**, 2167 (2017).

[17] S. Choi, S. Johnston, W.-J. Jang, K. Koepernik, K. Nakatsukasa, J. M. Ok, H.-J. Lee, H. W. Choi, A. T. Lee, A. Akbari, Y. K. Semertzidis, Y. Bang, J. S. Kim, and J. Lee, Phys. Rev. Lett. **119**, 107003 (2017).

[18] S. Choi, H. J. Choi, J. M. Ok, Y. Lee, W.-J. Jang, A. T. Lee, Y. Kuk, S. B. Lee, A. J. Heinrich, S.-W. Cheong, Y. Bang, S. Johnston, J. S. Kim, and J. Lee, Phys. Rev. Lett. **119**, 227001 (2017).

[19] H. Nakamura and M. Machida, Phys. Rev. B **82**, 094503 (2010).

[20] J. M. Ok, S. Na, and J. S. Kim, Prog. Supercond. Cryog. **20**, 28 (2018).

[21] T. Qian, N. Xu, Y.-B. Shi, K. Nakayama, P. Richard, T. Kawahara, T. Sato, T. Takahashi, M. Neupane, Y.-M. Xu, X.-P. Wang, G. Xu, X. Dai, Z. Fang, P. Cheng, H.-H. Wen, and H. Ding, Phys. Rev. B **83**, 140513(R) (2011).

[22] Y. K. Kim, Y. Y. Koh, W. S. Kyung, G. R. Han, B. Lee, K. H. Kim, J. M. Ok, J. S. Kim, M. Arita, K. Shimada, H. Namatame, M. Taniguchi, S.-K. Mo, and C. Kim, Phys. Rev. B **92**, 041116(R) (2015).

[23] G. H. Cao, Z. Ma, C. Wang, Y. Sun, J. Bao, S. Jiang, Y. Luo, C. Feng, Y. Zhou, Z. Xie, F. Hu, S. Wei, I. Nowik, I. Felner, L. Zhang, Z. Xu, and F. C. Zhang, Phys. Rev. B **82**, 104518 (2010).

[24] K. Ueshima, F. Han, X. Zhu, H.-H. Wen, S. Kawasaki, and G. Q. Zheng, Phys. Rev. B **89**, 184506 (2014).

[25] A. S. Sefat, D. J. Singh, V. O. Garlea, Y. L. Zuev, M. A. McGuire, and B. C. Sales, Phys. C (Amsterdam, Neth.) **471**, 143 (2011).

[26] S. Tatematsu, E. Satomi, Y. Kobayashi, and M. Sato, J. Phys. Soc. Jpn. **79**, 123712 (2010).

[27] S. Kim, J. M. Ok, H. Oh, C. Kwon, Y. Zhang, J. D. Denlinger, S.-K. Mo, F. Wolff-Fabrix, E. Kampert, E. Moon, C. Kim,

J. S. Kim, and Y. K. Kim, Proc. Natl. Acad. Sci. USA **118**, e2105190118 (2021).
[28] R. C. Che, F. Han, C. Y. Liang, X. B. Zhao, and H. H. Wen, Phys. Rev. B **90**, 104503 (2014).
[29] See Supplemental Material at http://link.aps.org/supplemental/10.1103/PhysRevB.105.214505 for additional information regarding the Hall effect and upper critical fields of $Sr_2VO_{3-\delta}FeAs$ in comparison with other FeSCs.
[30] S. Kasahara, K. Hashimoto, H. Ikeda, T. Terashima, Y. Matsuda, and T. Shibauchi, Phys. Rev. B **85**, 060503(R) (2012).
[31] F. Rullier-Albenque, D. Colson, A. Forget, P. Thuery, and S. Poissonnet, Phys. Rev. B **81**, 224503 (2010).
[32] L. S. Farrar, M. Bristow, A. A. Haghighirad, A. McCollam, S. J. Bending, and A. I. Coldea, npj Quantum Mater. **5**, 29 (2020).
[33] R. X. Cao, J. Dong, Q. L. Wang, Y. J. Yang, C. Zhao, X. H. Zeng, D. A. Chareev, A. N. Vasiliev, B. Wu, and G. Wu, AIP Adv. **9**, 045220 (2019).
[34] S. Ghannadzadeh, J. D. Wright, F. R. Foronda, S. J. Blundell, S. J. Clarke, and P. A. Goddard, Phys. Rev. B **89**, 054502 (2014).
[35] S. Takeshita and R. Kadono, New J. Phys. **11**, 035006 (2009).
[36] M. Nakajima, S. Ishida, T. Tanaka, K. Kihou, Y. Tomioka, T. Saito, C. H. Lee, H. Fukazawa, Y. Kohori, T. Kakeshita, A. Iyo, T. Ito, H. Eisaki, and S. Uchida, Sci. Rep. **4**, 5873 (2015).
[37] I. Pallecchi, C. Tarantini, Y. Shen, R. K. Singh, N. Newman, P. Cheng, Y. Jia, H.-H. Wen, and M. Putti, Supercond. Sci. Technol. **31**, 034007 (2018).
[38] K. Cho, H. Kim, M. A. Tanatar, Y. J. Song, Y. S. Kwon, W. A. Coniglio, C. C. Agosta, A. Gurevich, and R. Prozorov, Phys. Rev. B **83**, 060502(R) (2011).
[39] D. A. Zocco, K. Grube, F. Eilers, T. Wolf, and H. v. Löhneysen, Phys. Rev. Lett. **111**, 057007 (2013).
[40] C.-w. Cho, J. H. Yang, N. F. Q. Yuan, J. Shen, T. Wolf, and R. Lortz, Phys. Rev. Lett. **119**, 217002 (2017).
[41] H. Lei, R. Hu, E. S. Choi, J. B. Warren, and C. Petrovic, Phys. Rev. B **81**, 094518 (2010).
[42] S. A. Baily, Y. Kohama, H. Hiramatsu, B. Maiorov, F. F. Balakirev, M. Hirano, and H. Hosono, Phys. Rev. Lett. **102**, 117004 (2009).
[43] M. Fang, J. Yang, F. F. Balakirev, Y. Kohama, J. Singleton, B. Qian, Z. Q. Mao, H. Wang, and H. Q. Yuan, Phys. Rev. B **81**, 020509(R) (2010).
[44] S. K. Goh, Y. Nakai, K. Ishida, L. E. Klintberg, Y. Ihara, S. Kasahara, T. Shibauchi, Y. Matsuda, and T. Terashima, Phys. Rev. B **82**, 094502 (2010).
[45] L. Jiao, J. L. Zhang, F. F. Balakirev, G. F. Chen, J. L. Luo, N. L. Wang, and H. Q. Yuan, J. Phys. Chem. Solids **72**, 423 (2011).
[46] F. Rullier-Albenque, D. Colson, A. Forget, and H. Alloul, Phys. Rev. Lett. **109**, 187005 (2012).
[47] M. D. Watson, T. Yamashita, S. Kasahara, W. Knafo, M. Nardone, J. Beard, F. Hardy, A. McCollam, A. Narayanan, S. F. Blake, T. Wolf, A. A. Haghighirad, C. Meingast, A. J. Schofield, H. von Lohneysen, Y. Matsuda, A. I. Coldea, and T. Shibauchi, Phys. Rev. Lett. **115**, 027006 (2015).
[48] S. Ishida, T. Liang, M. Nakajima, K. Kihou, C. H. Lee, A. Iyo, H. Eisaki, T. Kakeshita, T. Kida, M. Hagiwara, Y. Tomioka, T. Ito, and S. Uchida, Phys. Rev. B **84**, 184514 (2011).
[49] X. Xing, W. Zhou, N. Zhou, F. Yuan, Y. Pan, H. Zhao, X. Xu, and Z. Shi, Supercond. Sci. Technol. **29**, 055005 (2016).
[50] G. F. Chen, W. Z. Hu, J. L. Luo, and N. L. Wang, Phys. Rev. Lett. **102**, 227004 (2009).
[51] J. P. Peña, M. M. Piva, P. F. S. Rosa, P. G. Pagliuso, C. Adriano, T. Grant, Z. Fisk, E. Baggio-Saitovitch, and P. Pureur, Phys. Rev. B **97**, 104502 (2018).
[52] X. Zhu, H. Yang, L. Fang, G. Mu, and H. H. Wen, Supercond. Sci. Technol. **21**, 105001 (2008).
[53] M. Kano, Y. Kohama, D. Graf, F. Balakirev, A. S. Sefat, M. A. McGuire, B. C. Sales, D. Mandrus, and S. W. Tozer, J. Phys. Soc. Jpn. **78**, 084719 (2009).
[54] J. Jaroszynski, F. Hunte, L. Balicas, Y. J. Jo, I. Raičević, A. Gurevich, D. C. Larbalestier, F. F. Balakirev, L. Fang, P. Cheng, Y. Jia, and H. H. Wen, Phys. Rev. B **78**, 174523 (2008).
[55] M. D. Watson, A. McCollam, S. F. Blake, D. Vignolles, L. Drigo, I. I. Mazin, D. Guterding, H. O. Jeschke, R. Valentí, N. Ni, R. Cava, and A. I. Coldea, Phys. Rev. B **89**, 205136 (2014).
[56] E. Mun, N. Ni, J. M. Allred, R. J. Cava, O. Ayala, R. D. McDonald, N. Harrison, and V. S. Zapf, Phys. Rev. B **85**, 100502(R) (2012).
[57] X. Xing, W. Zhou, J. Wang, Z. Zhu, Y. Zhang, N. Zhou, B. Qian, X. Xu, and Z. Shi, Sci. Rep. **7**, 45943 (2017).
[58] L. Jiao, Y. Kohama, J. L. Zhang, H. D. Wang, B. Maiorov, F. F. Balakirev, Y. Chen, L. N. Wang, T. Shang, M. H. Fang, and H. Q. Yuan, Phys. Rev. B **85**, 064513 (2012).
[59] H.-S. Lee, M. Bartkowiak, J.-H. Park, J.-Y. Lee, J.-Y. Kim, N.-H. Sung, B. K. Cho, C.-U. Jung, J. S. Kim, and H.-J. Lee, Phys. Rev. B **80**, 144512 (2009).
[60] J. M. Ok, C. I. Kwon, Y. Kohama, J. S. You, S. K. Park, J. H. Kim, Y. J. Jo, E. S. Choi, K. Kindo, W. Kang, K.-S. Kim, E. G. Moon, A. Gurevich, and J. S. Kim, Phys. Rev. B **101**, 224509 (2020).
[61] C. I. Kwon, J. M. Ok, and J. S. Kim, Prog. Supercond. Cryog. **16**, 26 (2014).
[62] J. L. Zhang, L. Jiao, F. F. Balakirev, X. C. Wang, C. Q. Jin, and H. Q. Yuan, Phys. Rev. B **83**, 174506 (2011).
[63] J. Xing, B. Shen, B. Zeng, J. Liu, X. Ding, Z. Wang, H. Yang, and H.-H. Wen, Sci. China: Phys., Mech. Astron. **55**, 2259 (2012).
[64] N. Kurita, M. Kimata, K. Kodama, A. Harada, M. Tomita, H. S. Suzuki, T. Matsumoto, K. Murata, S. Uji, and T. Terashima, Phys. Rev. B **88**, 224510 (2013).
[65] A. Gurevich, Rep. Prog. Phys. **74**, 124501 (2011).
[66] J. L. Zhang, L. Liao, Y. Chen, and H. Q. Yuan, Front. Phys. **6**, 463 (2011).
[67] R. Hu, E. D. Mun, M. M. Altarawneh, C. H. Mielke, V. S. Zapf, S. L. Bud'ko, and P. C. Canfield, Phys. Rev. B **85**, 064511 (2012).
[68] F. Hunte, J. Jaroszynski, A. Gurevich, D. C. Larbalestier, R. Jin, A. S. Sefat, M. A. McGuire, B. C. Sales, D. K. Christen, and D. Mandrus, Nature (London) **453**, 903 (2008).
[69] Y. Ma, Q. Ji, K. Hu, B. Gao, W. Li, G. Mu, and X. Xie, Supercond. Sci. Technol. **30**, 074003 (2017).
[70] T. Wang, C. Zhang, L. Xu, J. Wang, S. Jiang, Z. Zhu, Z. Wang, J. Chu, J. Feng, L. Wang, W. Li, T. Hu, X. Liu, and G. Mu, Sci. China: Phys.. Mech. Astron. **63**, 227412 (2020)
[71] Z. K. Liu, M. Yi, Y. Zhang, J. Hu, R. Yu, J.-X. Zhu, R.-H. He, Y. L. Chen, M. Hashimoto, R. G. Moore, S.-K. Mo, Z. Hussain, Q. Si, Z. Q. Mao, D. H. Lu, and Z.-X. Shen, Phys. Rev. B **92**, 235138 (2015).

[72] H. Ding, K. Nakayama, P. Richard, S. Souma, T. Sato, T. Takahashi, M. Neupane, Y. M. Xu, Z. H. Pan, A. V. Fedorov, Z. Wang, X. Dai, Z. Fang, G. F. Chen, J. L. Luo, and N. L. Wang, J. Phys.: Condens. Matter **23**, 135701 (2011).
[73] B. Mansart, E. Papalazarou, M. F. Jensen, V. Brouet, L. Petaccia, L. de' Medici, G. Sangiovanni, F. Rullier-Albenque, A. Forget, D. Colson, and M. Marsi, Phys. Rev. B **85**, 144508 (2012).
[74] Y. Zhang, J. Wei, H. W. Ou, J. F. Zhao, B. Zhou, F. Chen, M. Xu, C. He, G. Wu, H. Chen, M. Arita, K. Shimada, H. Namatame, M. Taniguchi, X. H. Chen, and D. L. Feng, Phys. Rev. Lett. **102**, 127003 (2009).
[75] S. V. Borisenko, D. V. Evtushinsky, Z.-H. Liu, I. Morozov, R. Kappenberger, S. Wurmehl, B. Buchner, A. N. Yaresko, T. K. Kim, M. Hoesch, T. Wolf, and N. D. Zhigadlo, Nat. Phys. **12**, 311 (2016).
[76] L. X. Yang, B. P. Xie, Y. Zhang, C. He, Q. Q. Ge, X. F. Wang, X. H. Chen, M. Arita, J. Jiang, K. Shimada, M. Taniguchi, I. Vobornik, G. Rossi, J. P. Hu, D. H. Lu, Z. X. Shen, Z. Y. Lu, and D. L. Feng, Phys. Rev. B **82**, 104519 (2010).
[77] D. H. Lu, M. Yi, S.-K. Mo, A. S. Erickson, J. Analytis, J.-H. Chu, D. J. Singh, Z. Hussain, T. H. Geballe, I. R. Fisher, and Z.-X. Shen, Nature (London) **455**, 81 (2008).
[78] C. Liu *et al.*Phys. C (Amsterdam, Neth.) **469**, 491 (2009).
[79] S. Jiang, L. Liu, M. Schutt, A. M. Hallas, B. Shen, W. Tian, E. Emmanouilidou, A. Shi, G. M. Luke, Y. J. Uemura, R. M. Fernandes, and N. Ni, Phys. Rev. B **93**, 174513 (2016).
[80] A. Gurevich, Phys. Rev. B **67**, 184515 (2003).
[81] N. Kurita, M. Kimata, K. Kodama, A. Harada, M. Tomita, H. S. Suzuki, T. Matsumoto, K. Murata, S. Uji, and T. Terashima, Phys. Rev. B **83**, 100501(R) (2011).
[82] V. Jaccarino and M. Peter, Phys. Rev. Lett. **9**, 290 (1962).
[83] K. Maki, Phys. Rev. **148**, 362 (1966).
[84] S. Khim, B. Lee, J. W. Kim, E. S. Choi, G. R. Stewart, and K. H. Kim, Phys. Rev. B **84**, 104502 (2011).
[85] T. Terashima, M. Kimata, H. Satsukawa, A. Harada, K. Hazama, S. Uji, H. Harima, G.-F. Chen, J.-L. Luo, and N.-L. Wang, J. Phys. Soc. Jpn. **78**, 063702 (2009)
[86] M. Decroux, S. E. Lambert, M. S. Torikachvili, M. B. Maple, R. P. Guertin, L. D. Woolf, and R. Baillif, Phys. Rev. Lett. **52**, 1563 (1984).
[87] H. W. Meul, C. Rossel, M. Decroux, O. Fischer, G. Remenyi, and A. Briggs, Phys. Rev. Lett. **53**, 497 (1984).
[88] S. Uji, H. Shinagawa, T. Terashima, T. Yakabe, Y. Terai, M. Tokumoto, A. Kobayashi, H. Tanaka, and H. Kobayashi, Nature (London) **410**, 908 (2001).
[89] K. Hiraki, H. Mayaffre, M. Horvatic, C. Berthier, S. Uji, T. Yamaguchi, H. Tanaka, A. Kobayashi, H. Kobayashi, and T. Takahashi, J. Phys. Soc. Jpn. **76**, 124708 (2007).
[90] S. Zapf and M. Dressel, Rep. Prog. Phys. **80**, 016501 (2017)
[91] I. I. Mazin, Phys. Rev. B **81**, 020507 (2010).